Learning sculpts the spontaneous activity of the resting human brain

Christopher M. Lewis[a,b,1], Antonello Baldassarre[a,b,1], Giorgia Committeri[a,b], Gian Luca Romani[a,b], and Maurizio Corbetta[a,b,c,2]

[a]Department of Clinical Sciences and Bioimaging, G. D'Annunzio University, Via dei Vestini 33, 66100, Chieti, Italy; [b]Institute for Advanced Biomedical Technologies, G. D'Annunzio Foundation, Via dei Vestini 33, 66100, Chieti, Italy; and [c]Departments of Neurology, Radiology, Anatomy, and Neurobiology, Washington University School of Medicine, 4525 Scott Avenue, 63110, St. Louis, MO

The brain is not a passive sensory-motor analyzer driven by environmental stimuli, but actively maintains ongoing representations that may be involved in the coding of expected sensory stimuli, prospective motor responses, and prior experience. Spontaneous cortical activity has been proposed to play an important part in maintaining these ongoing, internal representations, although its functional role is not well understood. One spontaneous signal being intensely investigated in the human brain is the interregional temporal correlation of the blood-oxygen level-dependent (BOLD) signal recorded at rest by functional MRI (functional connectivity-by-MRI, fcMRI, or BOLD connectivity). This signal is intrinsic and coherent within a number of distributed networks whose topography closely resembles that of functional networks recruited during tasks. While it is apparent that fcMRI networks reflect anatomical connectivity, it is less clear whether they have any dynamic functional importance. Here, we demonstrate that visual perceptual learning, an example of adult neural plasticity, modifies the resting covariance structure of spontaneous activity between networks engaged by the task. Specifically, after intense training on a shape-identification task constrained to one visual quadrant, resting BOLD functional connectivity and directed mutual interaction between trained visual cortex and frontal-parietal areas involved in the control of spatial attention were significantly modified. Critically, these changes correlated with the degree of perceptual learning. We conclude that functional connectivity serves a dynamic role in brain function, supporting the consolidation of previous experience.

fMRI | functional connectivity | perceptual learning | resting state

Spontaneous neural activity utilizes the majority of the brain's energy budget, but its function remains mysterious (1–8). At the level of single neurons, embedded in the local circuitry of a cortical area, spontaneous activity has been shown to emulate the pattern of activity evoked by the neuron's optimal stimulus, suggesting that at least at this level of description, spontaneous activity is likely to reflect the history of coactivation within local networks (9). At the level of distributed cortical systems, spontaneous activity measured by blood-oxygen level-dependent (BOLD) functional MRI (fMRI) exhibits covariance structures (or functional connectivity) at ultra-slow frequencies (<0.1 Hz) that are stable across a wide range of behavioral states (anesthesia, task performance, resting wakefulness, and sleep) (10, 11). The topography of BOLD functional connectivity is compatible with both the underlying structural connectivity of the cortex and the functional anatomy of systems engaged by a broad range of tasks (12–16).

Studies have suggested that BOLD functional connectivity is largely a physiological marker of anatomical connections or a correlate of intrinsic vascular dynamics without functional or behavioral significance (17). This hypothesis is consistent with the stability of functional connectivity independent of behavioral state, as well as the maturation of stable networks from childhood to adulthood in parallel with the myelination of the brain's white matter (18). However, other evidence indicates that the strength of correlation within a network can be related to

individual differences in cognitive function (11, 19, 20), that spontaneous activity can account for the variability of task-evoked responses (21), and that the disruption of BOLD connectivity in the absence of structural damage is associated to neurological deficits (22). These findings suggest that spontaneous functional connectivity may encode or support the encoding of behaviorally relevant information.

Based on this evidence, we sought to demonstrate that prior experience (i.e., the history of network activation) changes resting functional connectivity in a behaviorally specific manner. We acquired resting fMRI before and after intense training on a difficult shape-discrimination task at a specific location in the visual field. If functional connectivity is related to the neuronal changes associated with perceptual learning, then training-specific plasticity should be exhibited.

Results

Perceptual Learning Training. For several days, 14 healthy subjects were trained to attend to the left lower visual quadrant and report the presence or absence of a target shape (an inverted T) in a circular array of distracters (differently oriented Ts). Stimuli were presented rapidly (150 ms) to prevent eye movement. Eye movements were recorded and monitored to ensure fixation (see Fig. S1). The target shape appeared randomly in 1 of 3 locations in the left lower (trained) visual quadrant, while the distracters appeared in the other 3 (untrained) quadrants (Fig. 1A). An average of 5,600 practice trials were necessary to reach a threshold of 80% accuracy in at least 10 consecutive blocks of trials (see Fig. 1B for a representative psychophysical curve; see Table S1 for individual results). Perceptual learning was specific for the trained shape and trained quadrant, and did not generalize to other quadrants and orientations (Fig. 1C). These behavioral data confirm the well-known retinotopic and orientation specificity of perceptual learning (23, 24).

Retinotopic Localizer. Before any exposure to the task, we identified the regions of visual cortex that differentially responded to the stimulus array presented in the 4 visual quadrants during a passive-stimulation condition (Fig. S2A). This was done to avoid any influence of training on the baseline responsiveness of different portions of visual cortex to the localizer stimuli.

Task-Evoked Modulation in Visual Cortex. Upon completion of the behavioral training, we measured the effect of learning on re-
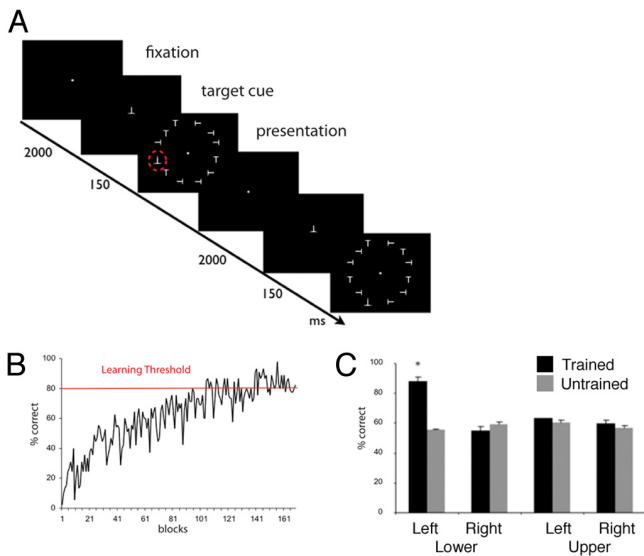
Fig. 1. Behavioral training and psychophysics results. (*A*) Illustration of timeline for 2 trials. On each trial subjects fixated a central spot for 200 ms (fixation), after which the target shape (an inverted T) was presented at the center of the screen for 2,000 ms (target presentation); finally, an array of 12 stimuli, differently oriented Ts (distracters) with or without an inverted T (target), was briefly flashed for 150 ms (array presentation). Subjects attended to the lower left visual quadrant and indicated the presence or absence of the target shape (*red* ○) in that visual quadrant (○ was not present in the display; see *SI Methods* for more details). (*B*) Example of a single subject's learning curve. Each block contains 45 trials. The red line indicates a learning threshold of 80% accuracy in 10 consecutive trial blocks. (*C*) Psychophysical comparison of accuracy in all quadrants. In a control session at the end of training, subjects were asked to discriminate between trained and uniquely shaped orientations in all visual quadrants. A repeated-measure ANOVA, with shape (trained, untrained) and quadrant (trained *Lower Left*, *Lower Right*, *Upper Left*, *Upper Right*) as factors, showed a significant main effect of quadrant [F (3, 21) = 3.52, $P < 0.05$], and a significant interaction of shape by quadrant [F (3, 21) = 8.49, $P < 0.001$]. Posthoc contrasts (Newman-Keuls test) showed that performance in the trained condition (trained shape in the trained visual quadrant) was better with respect to any other condition. (*n* = 6; Error bars, ± SEM; ∗, $P < 0.05$).

sponses in the visual cortex by comparing blocks of trials in which subjects discriminated stimulus arrays containing either the trained target shape or an untrained target shape (right/left tilted T). The target stimuli were always presented in the trained visual quadrant (Fig. S3). As in the behavioral training sessions, performance was higher for trained than untrained targets (see Fig. S3).

The effect of learning (i.e., a differential response to trained versus untrained targets) was measured in the regions of interest in the visual cortex defined during the localizer scans. The response to untrained shapes was attenuated (as compared to trained ones) in the right dorsal cortex corresponding to the attended left lower quadrant, but not in the ventral visual cortex corresponding to the nonattended upper visual quadrants (Fig. 2). This pattern indicates topographic and shape specificity of the learning-dependent modulation. There was also a significant difference between trained and untrained shapes in the left dorsal cortex corresponding to the homologous (untrained) right lower quadrant (see Fig. 2) [condition (trained, untrained) by quadrant (lower left, lower right, upper left, upper right) interaction [F (3, 33) = 7,75; $P = 0.0005$; posthoc (Newman-Keuls test) for lower left, $P < 0.0002$; for lower right $P < 0.001$]]. The modulation localized to right dorsal V1 to V3 and V3A to LO, and left V1 to V3 on the basis of a population atlas of human visual areas (25) (see Fig. 2, Table S2). In addition, the response to trained shapes was stronger in the contra-lateral (trained)

Fig. 2. Task-evoked modulation of the visual cortex after perceptual learning. (*Center*) Stimulus array with colored squares (not present in real display) indicating 4 visual quadrants. (*Flat maps*) visual cortex ROIs obtained from passive localizer scans by stimulating one quadrant at a time (Fig. S2). ROIs are projected onto a flattened representation of the posterior occipital cortex using the PALS (population-average, landmark, and surface-based) atlas (25). Bar plots: % signal change of BOLD in each quadrant when attending to the lower left quadrant and discriminating trained or untrained targets. Note that all 4 quadrants of the visual cortex were stimulated by the stimulus array, but only the trained visual quadrant in the right dorsal and the homologous area in left dorsal visual cortex show a shape-specific modulation. (Posthoc Newman-Keuls test, *n* = 12; Error bars, ± SEM; ∗, P < 0.05).

than ipsi-lateral (untrained) dorsal cortex ($P < 0.0002$), consistent with a shape-specific modulation.

A separate whole brain voxel-wise analysis provided further support for topographic and shape specificity. In this analysis, the only significant portion of visual cortex showing preferential activity for trained vs. untrained shape blocks was localized in right dorsal cortex (Fig. 3*A*) in 2 regions (V2/V3 and LO) that were contralateral to the attended left lower quadrant, and within the borders of the regions responding to the retinotopic stimulus (Fig. S2*C*).

These findings are in line with previous studies, showing that orientation-specific learning changes the tuning properties of neurons in the early visual cortex, and increases the fMRI signal to trained vs. untrained shapes (26). Here, we show that modulation in the visual cortex is topographically and shape specific and mainly consists of the filtering of sensory-evoked responses to novel (untrained) shapes in the attended quadrant, which presumably leads to a more specific response to the trained shape. The presence of training-related modulation in the visual cortex homologous to the representation of the trained quadrant is not surprising in light of several recent fMRI studies (27, 28). These studies suggest that modulations in the visual cortex are not restricted to attended locations, as previously believed, but extend to unattended locations, especially those in the opposite hemisphere homologous to the attended ones. This pattern reflects a specific computational mechanism for coding the locus of attention in a cortical map based on activity difference between attended and unattended locations (27, 29).

Task-Evoked Activity Outside the Occipital Cortex. A number of parietal and frontal regions responded more strongly during untrained as compared to trained shape blocks (see *blue regions* in Fig. 3*A*; Table S3). These regions correspond to the dorsal fronto-parietal attention network (30), the source of spatially selective attention biases to the visual cortex (31), as well as portions of a core control network (32) involved in task set maintenance and error tracking. The stronger activation for novel shape orientation likely reflects a higher degree of attention engagement, similar to that occuring during early training, as opposed to when the shape orientation is familiar. Finally, a separate set of cortical regions was more strongly deactivated during untrained as opposed to trained shape blocks (see *orange regions* in Fig. 3*A*). These regions corre-
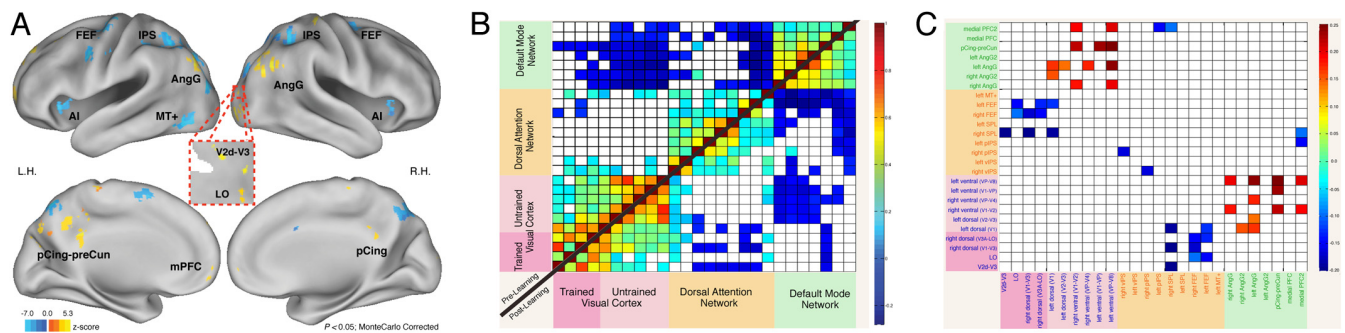
Fig. 3. Whole-brain task-evoked modulation and spontaneous functional connectivity after perceptual learning. (*A*) Whole-brain voxel-wise *z*-map of trained minus untrained shape conditions, corrected for multiple comparisons (Monte-Carlo, *P* < 0.05) and projected onto an inflated representation of the PALS atlas. Central inset shows activation in the right dorsal visual cortex projected onto a flattened representation of the occipital lobe. Blue regions represent response for untrained > trained; orange regions represent response for trained > untrained. *n* = 12. (*B*) Pre- and postlearning spontaneous fcMRI. Color bar indicates *z*-transformed correlation values for each region pair, positive for red cells and negative for blue cells. Note stability of the correlation matrix across sessions (separated by >1 week), indicating that within-network functional connectivity is very stable over time (*n* = 14). (*C*) Post- minus prelearning changes in spontaneous fcMRI. Correlation matrix (Fisher *z*-transformed Pearson coefficient) of all possible ROI pairs in the visual cortex, dorsal attention network (DAN), and default mode network (DMN). Color bar indicates post- minus prelearning *z*-transformed correlation values (rest 2 – rest 1 scans) for each region pair. Blue cells represent significant correlation difference between dorsal attention and trained visual cortex ROIs (*t* test, *P* < 0.03, corrected for multiple comparisons): prelearning > postlearning. Red cells represent significant correlation difference between default network and untrained visual cortex ROIs, postlearning > prelearning; *n* = 14.

spond to the default mode network (33, 34), in which previous studies have also reported deactivations that are attention-load dependent (35, 36).

In summary, learning-induced specific modulation of task-evoked activity in the visual cortex and higher order control regions of the attention, core, and default networks, is consistent with the essential role of visuo-spatial attention in perceptual learning (23, 24), the retinotopic organization of its top-down influence on visual areas (37), and its role in filtering distracters (38).

Functional Connectivity Changes Between Networks. Next, we examined the effect of perceptual learning on the patterns of resting functional connectivity in the brain networks recruited by the task (dorsal attention, default, and visual). Two sets of fMRI resting-state scans, in which subjects simply maintained visual fixation, were acquired before and after behavioral training to measure the spontaneous coherence of BOLD signal fluctuations between task regions. The prelearning scans were obtained before any exposure to the task, while the postlearning scans were obtained after measuring the effects of learning on task-evoked activity. BOLD signal time courses were extracted from all task-specific and localizer regions, and temporal correlation was computed pair-wise during each rest period (functional connectivity or fcMRI).

Functional connectivity was stronger within-network than across-networks and the overall topography of correlations was consistent over time (10, 39) (Fig. 3*B*). Notably, significant correlation differences before and after learning were detected between networks, but not within the network. After learning, the functional connectivity between trained visual cortex and dorsal attention regions [left and right frontal eye field (FEF); right superior parietal lobule] became more negatively correlated (Fig. 3*C* and Fig. 4*A*). Additionally, functional connectivity between the untrained visual cortex and several default regions [left medial prefrontal; right angular gyrus (AngG); right and left posterior cingulate] became less negatively correlated (see Fig. 3*C* and Fig. 4*B*). Finally, in the left dorsal visual cortex (i.e., corresponding to the lower right visual quadrant homologous to the trained quadrant, and which showed learning-related evoked BOLD change) both modulations occurred: that is, an increased negative correlation with dorsal attention regions and a decreased negative correlation with default regions (Fig. S4*A*).

A number of control analyses (See *SI Methods*) showed that: (*i*) functional connectivity changes were specific to the visual system and did not extend to the auditory system (Fig. S5*A*); (*ii*) other networks recruited during visual perceptual training (motor, core) also showed topographically specific learning-dependent changes in functional connectivity (Fig. S5*B*); and (*iii*) functional connectivity changes could not be explained by covert task rehearsal (Fig. S5*C*). These findings clearly demon-
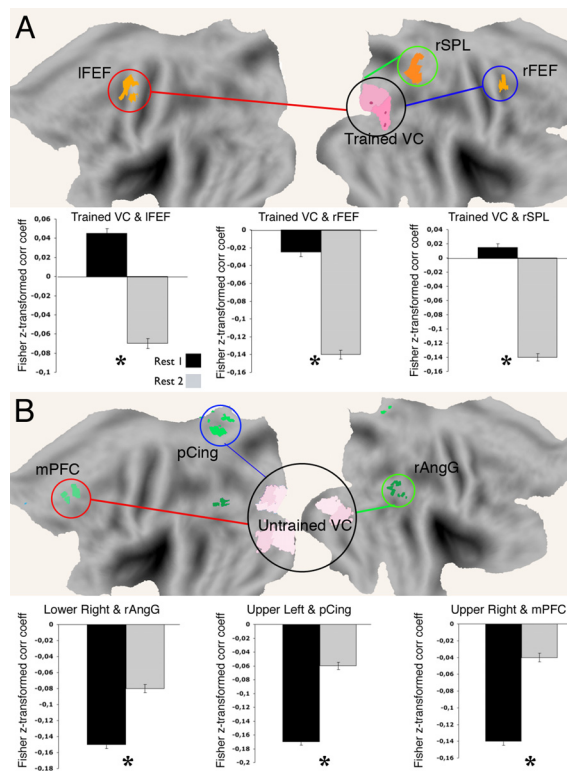

Fig. 4. Modulation of spontaneous functional connectivity after perceptual learning. Flattened brain representation with ROIs in trained visual cortex and dorsal attention network (*A*) and in untrained visual cortex and default network (*B*). Bar graphs report correlation values (*r*) between trained visual cortex and dorsal attention ROIs and untrained visual cortices and default network ROIs before (*black*) and after (*gray*) perceptual learning. *n* = 14. *r*, Pearson correlation coefficient; Student's *t* test, 2 tails, *P* < 0.05; error bars ± SEM.
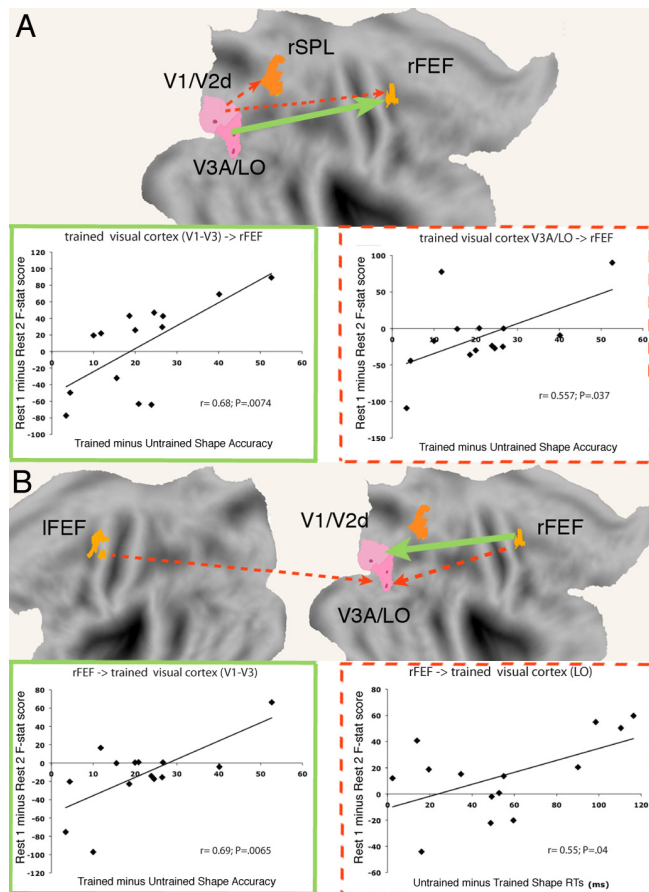
Fig. 5. Modulation of GC after perceptual learning. Changes in GC directional modulation after learning that correlate with behavioral performance. (A) Bottom-up GC change. Scatter plots show the positive correlation between bottom-up GC modulation measured as F-statistic score (y-axis) and behavioral improvement measured as trained minus untrained shape accuracy score (x-axis). (r = 0.68, P = 0.0074 for right V1/V2d/V3 → right FEF; r = 0.557, P = 0.037 for V3A/LO → right FEF). (B) Top-down GC change. Scatter plots show the positive correlation between top-down GC modulation measured as F-statistic score (y-axis) and behavioral improvement measured as trained minus untrained shape accuracy score (green) or untrained minus trained shape reaction time score (x-axis). (r = 0.687, P = 0.0065 for right FEF → right V1/V2d/V3; r = 0.55, P = 0.0409 for right FEF → right LO). Green arrows and outlines indicate increased GC (postlearning > prelearning); red dashed arrows and outlines indicate decreased GC (prelearning > postlearning). n = 14.

strate that perceptual learning altered the spontaneous functional connectivity between visual cortex and task networks.

Changes in Directed Mutual Information. Not only did the total amount of temporal correlation change with learning between visual, attention, and default networks, but so did the degree and pattern of directed interaction, as expressed by Granger causality (GC) (40). Two regions are said to display Granger causality when the autoregressive temporal model for one region's time series is improved by including previous time points from the other region. This measure can be calculated in a top-down direction (e.g., from dorsal attention to visual regions) and in a bottom-up direction (e.g., from visual to dorsal attention regions). Comparing pre- to postlearning spontaneous GC, we observed a relative increase in the bottom-up direction from intermediate level visual areas (V3A–LO) to FEF, but a relative decrease for low-level visual areas (V1d–V3) to FEF bilaterally (Fig. 5A and Fig. S6). Conversely, in the top-down direction, we measured a relative decrease from right FEF to V3A-LO, but a relative increase from right FEF to V1d-V3 (see Fig. 5C and Fig. S6).

That learning-dependent changes in top-down and bottom-up GC match across visual areas is significant because the analysis was performed independently for different region pairs and directions. The pattern suggests that interaction between regions in the dorsal attention network is shifting and differentially moving across the visual hierarchy before and after learning.

Behavioral Correlations. Finally, we observed a number of interesting correlations between learning-dependent changes in task-evoked activity, functional connectivity, and GC and behavioral performance. First, subjects with higher sensitivity for trained shapes (trained-untrained accuracy) also showed stronger task-evoked modulation in the trained quadrant (Fig. S7) (r = 0.7, P = 0.006 for lower left; P > 0.05 for all other quadrants). Second, subjects who responded more quickly to familiar shapes (larger untrained-trained reaction times) developed more negative correlation after learning between trained visual cortex and dorsal attention regions (r = 0.72, P = 0.0038 for right FEF-trained visual cortex; r = 0.51, P = 0.059 for left FEF-trained visual cortex; P > 0.05 for all other quadrants) (Fig. S4C). Lastly, the degree of GC modulation between the trained visual cortex and dorsal attention network also correlated with behavior. Subjects with greater changes in GC between the 2 networks, in both top-down and bottom-up directions, did not perform as well as subjects in whom GC modifications were less pronounced (see Fig. 5). This suggests 2 nonexclusive interpretations. First, performance could be better when minimal changes to directional network dynamics occur as a result of learning. For example, subjects who try harder may alter their functional architecture to a greater extent, while not necessarily achieving improved performance. Alternatively, performance may be better when, before learning, the brain already has a pattern of directional interaction between visual cortex and attention regions that is conducive to better performance.

Discussion

The preceding descriptions of learning-induced changes in resting functional connectivity powerfully demonstrate the dynamic nature of spontaneous BOLD coherence and suggest a role in brain function beyond an inert recapitulation of gross anatomy or intrinsic vascular dynamics. We show that prior experience in the form of visual perceptual learning can change the pattern of spontaneous cortical activity between different brain networks in specific ways. The networks that are recruited in the course of training show robust and specific learning-related modulation in resting BOLD connectivity. This provides strong support for the hypothesis that the coordinated activation of cortical networks during behavior shapes the organized pattern of correlated spontaneous activity at rest. By extension, functional networks observed in the adult brain are likely to reflect the patterned history of regional coactivation in the course of development and individual experience. Moreover, the colocalization of learning-dependent functional connectivity changes with task-evoked modulations, and their correlation with learning suggests that patterns of spontaneous activity influence the task-dependent recruitment of the same cortical circuits. We discuss first the interpretation and possible neural bases of observed changes in functional connectivity. Next, we consider their functional significance and relationship with task-driven activation.

The visual perceptual task used in this study was akin to an entirely new experience for our subjects. The acquisition of expertise was slow (thousands of trials) and required the development of an entirely new set of stimulus-response associations. In addition, subjects had to recruit/execute a number of operations during training, including shifts and maintenance of spatial attention to the left lower quadrant, development of a perceptual template for the target, and filtering of unattended information from the distractors. With time, subjects reported seeing the target shape effortlessly (as if it "pops-out" from the background). Prior neuroimaging studies have established that this task involves an interaction of the visual

cortex with fronto-parietal regions, with development of expertise being associated with sharpening of orientation tuning curves and fMRI response enhancement in the visual cortex, and less pronounced activation of higher-order control areas (26–30).

Here, we show that perceptual learning also entrains unique patterns of spontaneous activity in the same neural networks recruited by the task. It is as if learning sculpts the connectivity of existing functional networks. Specifically, trained visual cortex and fronto-parietal attention areas that were independent before training (i.e., resting correlation near zero) (see Fig. 4A) became negatively correlated after learning. Across subjects, more negative correlation corresponded with improved perceptual learning. While the precise definition of the underlying neural mechanisms will require more invasive recording, we interpret the negative correlation as reflecting the active (i.e., metabolically demanding) decoupling of fronto-parietal attention and occipital visual areas. This interpretation is consistent with the experience of perceptual learning: early in training, subjects detect the target only by paying close attention, whereas after learning the development of a target template in the visual cortex allows for more automatic and effortless discrimination that requires less on-line top-down control. This trained behavioral state corresponds to a state of anticorrelation between visual and attention regions. Anticorrelation in spontaneous BOLD activity may be related to antiphase changes in slow cortical potentials and gamma power (41–43), which may prevent the 2 systems from interfering with each other under task conditions. Analysis of large-scale neural network models indicates that spontaneous network anticorrelation is an efficient computational state to facilitate independent task recruitment and switching (44). This interpretation is also supported by the GC analysis. The increase in bottom-up drive from intermediate visual areas (V3A/LO), which are specialized in object and orientation discrimination (45), to higher-order visual areas (FEF) involved in decision-making, may reflect the adjustment of internetwork information flow facilitating more automatic detection of the target shape. Conversely, the increase in top-down drive from FEF to early visual areas (V1–V3) may correspond to the establishment of filtering mechanisms for unattended information in the trained quadrant. Similarly, the decrease in negative correlation between untrained portions of the visual cortex and regions of the DMN can be interpreted in this framework as the attenuation of a "filter" mechanism for unattended sensory information in the nontrained quadrants, which becomes less important as training progresses. We are unique in reporting topographically specific negative correlations between the visual cortex and the default network, and this finding links—more directly than any previous study (35, 36)—activity in this network to perceptual operations in contrast to prevalent views of its involvement in self-referential functions (theory of mind, episodic memory, internal thoughts, and so forth) (46).

Learning-dependent changes in spontaneous coherence also seem to have an impact on how the same circuits fire during the visual perceptual task. In the same quadrant of visual cortex in which we observed behaviorally significant postlearning modulation of task-evoked activity, we also measured behaviorally significant changes of resting-state fcMRI and directional interaction. The idea that the pattern of spontaneous activity constrains task-driven responses and behavioral output is consistent with other observations. For example, the phase of ultraslow EEG oscillations correlates with behavioral performance, suggesting a relationship between slow oscillations, task-driven responses, and behavioral output (47).

We conclude that spontaneous BOLD connectivity does not simply reflect the structure of the underlying anatomical circuitry, as has been well documented (16, 48, 49), but underlies functional links acting as a form of "system memory" that recapitulates the history of experience-driven coactivation on cortical circuitries. Our results in the perceptual domain closely match a recent report by

Albert et al. (50), who demonstrated increased functional connectivity in the motor system only when subjects learn a novel task, but not when they repeat a familiar task with the same intensity. This is a fundamental distinction because it suggests that functional connectivity encodes novel patterns of coactivation, possibly through the recruitment of specific synaptic mechanisms. For example, a recent study reported widespread enhancement of fMRI activity in hippocampus and connected cortical regions during microstimulation protocols that induce long-term potentiation (51). Perceptual learning may induce similar changes at the cortical level that are then manifested in modulation of both resting functional connectivity and task-evoked activity.

Finally, our results provide an intriguing perspective on the functional role of spontaneous coherence in cortical networks as identified by fMRI. This signal does not reflect a simple physiological marker of anatomical pathways, but has clear functional significance as it predicts cognitive performance (6, 20), behavioral deficits (22), and changes with learning (51). That the most relevant changes in our study occur between, rather than within, networks indicates that this signal may be especially important in linking large-scale cortical networks. This is also consistent with the observation that BOLD coherence is related to low frequency fluctuations of neuronal activity (42, 52) that are deemed more important for long-distance cortical communication (53). One hypothesis we favor is that spontaneously correlated networks represent preferential channels through which neuronal populations in different areas can communicate. The slow fluctuation of coherent activity can be thought of as a temporal scaffold that implements selection mechanisms similar to those described in the communication-through-coherence hypothesis (54). Accordingly, communication between distant cortical regions is enhanced by increasing the coherence of spontaneous oscillatory activity, which in turn facilitates the transfer of information coded in spike rates. Originally envisioned to explain synchronization in the gamma band, this hypothesis could be extended to account for the coupling of high frequencies to slow rhythms described in several recent studies (55, 56) and their relationship to behavior (47).

Methods

Subjects. Fourteen healthy, right-handed volunteers (7 females, aged 20 to 30) with no psychiatric or neurological disorders, and normal or corrected-to-normal vision, participated in the study after providing written informed consent. The University G. D'Annunzio of Chieti's Institutional Ethics Committee approved the experimental protocol.

Visual Stimuli. The stimulus array comprised 12 Ts arranged in an annulus of 5° radius and displayed across the 4 visual quadrants. The inverted T was the trained target shape, while differently oriented Ts were the distracters. Presentation timing was triggered by the acquisition of fMRI frames.

Behavioral Training. Subjects were trained with daily sessions to attend to the lower left visual quadrant and find the target shape among the distracters while maintaining central fixation. Training lasted from 2 to 9 days and continued until the level of performance was >80% in at least 10 consecutive blocks (57).

fMRI Procedure and Scanning. Before behavioral training, imaging data were acquired in a scanning session consisting of 6 runs of resting state, in which subjects were instructed to fixate a small cross under low-level illumination and to remain passive (free from pursuing focused thought), and 6 runs of a functional retinotopic localizer to identify voxels preferentially responding to each visual quadrant. When subjects reached the learning threshold, a second functional session was acquired with 6 resting state runs and 6 runs on the trained shape-identification task, each consisting of 5 trained and 5 untrained blocks alternated with 5 fixation blocks. More detailed information on MRI acquisition and processing parameters is in the *SI Methods*.

Behavioral Analysis. For each block, we recorded the number of positive responses (p) and the reaction time. Detailed discussion of behavioral measures we used is in the *SI Methods*.

Lewis et al.

Localizer and Shape Identification Task Data Processing. The BOLD time course at each voxel, for each subject, was subjected to a general linear model with an assumed response function using in-house software. Analysis details are in the *SI Methods*.

Regions of Interest Creation. Regions of interest (ROIs) were functionally defined for localizer and task data using an in-house clustering algorithm. ROIs were initially defined as 15-mm spheres centered on peaks (threshold between z-score 3 and -3); peaks within 15 mm of each other were consolidated into a single ROI.

fcMRI Data Analysis. For each subject and for each resting-state period (before and after training), BOLD time courses were extracted from localizer and task ROIs, the correlation matrix was calculated, and z-values were obtained using the Fisher transform. A t test across subjects was then used to threshold the mean correlation matrix ($P < 0.03$, Monte-Carlo corrected for multiple comparisons). We then computed the difference between the first and second rest session correlation matrices for each subject, and the paired t test between rest periods ($P < 0.03$, Monte-Carlo corrected for multiple comparisons) was used to threshold the mean-difference matrix. Information on preprocessing specific to functional connectivity analysis is in *SI Methods*.

Granger Analysis. For pairs of ROIs that showed a significant change in correlation between rest periods, we computed GC (37) F-statistics for each subject and each rest period using the Granger Test implementation in the Markov-Switching Bayesian Vector Autoregression Models Package (58) of the R Environment (59). We computed Order-1 bivariate Granger Tests for each ROI pair and obtained an F-statistic and *P*-score in each direction for time lag lengths between 1 and 10 MR frames. To investigate Granger directionality changes between rest periods, we computed the difference between F-statistics in the pre- and postlearning rest periods.

Behavior and Brain Activity Correlation. For each subject, we calculated measures of behavioral improvement (reaction time and accuracy, as described above) and then the percent BOLD change related to trained vs. untrained shape in the ROIs. We also computed for each subject and for each pair of ROIs significant differences of fcMRI and GC between resting states. Using a Pearson correlation coefficient we calculated the correlation between behavioral improvement and brain activity modulation (task evoked, spontaneous fcMRI, and GC).

1. Llinas R, Ribary U, Contreras D, Pedroarena C (1998) The neuronal basis for consciousness. *Philos Trans R Soc Lond B Biol Sci* 353:1841–1849.
2. Varela F, Lachaux J-P, Rodriguez E, Martinerie J (2001) The brainweb: Phase synchronization and large-scale integration. *Nat Rev Neurosci* 2:229–239.
3. Engel AK, Fries P, Singer W (2001) Dynamic predictions: Oscillations and synchrony in top-down processing. *Nat Rev Neurosci* 2:704–716.
4. Kenet T, Bibitchkov D, Tsodyks M, Grinvald A, Arieli A (2003) Spontaneously emerging cortical representations of visual attributes. *Nature* 425:954–956.
5. Raichle ME, Mintun MA (2006) Brain work and brain imaging. *Annu Rev Neurosci* 29:449–476.
6. Hampson M, Driesen NR, Skudlarski P, Gore JC, Constable RT (2006) Brain connectivity related to working memory performance. *J Neurosci* 26:13338–13343.
7. Raichle ME, Gusnard DA (2002) Appraising the brain's energy budget. *Proc Natl Acad Sci USA* 99:10237–10239.
8. Balduzzi D, Riedner BA, Tononi G (2008) A BOLD window into brain waves. *Proc Natl Acad Sci USA* 105:15641–15642.
9. Tsodyks M, Kenet T, Grinvald A, Arieli A (1999) Linking spontaneous activity of single cortical neurons and the underlying functional architecture. *Nature* 286:1943–1946.
10. Vincent JL, et al. (2007) Intrinsic functional architecture in the anaesthetized monkey brain. *Nature* 447:83–86.
11. Boly M, et al. (2008) Consciousness and cerebral baseline activity fluctuations. *Hum Brain Mapp* 29:868–874.
12. Biswal B, Yetkin F, Haughton V, Hyde J (1995) Functional connectivity in the motor cortex of resting human brain using echo-planar MRI. *Magn Reson Med* 34:537–541.
13. Greicius MD, Krasnow B, Reiss AL, Menon V (2003) Functional connectivity in the resting brain: A network analysis of the default mode hypothesis. *Proc Natl Acad Sci USA* 100:253–258.
14. De Luca M, Smith S, De Stefano N, Federico A, Matthews PM (2005) Blood oxygenation level dependent contrast resting state networks are relevant to functional activity in the neocortical sensorimotor system. *Exp Brain Res* 167:587–594.
15. Fox MD, et al. (2005) The human brain is intrinsically organized into dynamic, anticorrelated functional networks. *Proc Natl Acad Sci USA* 102:9673–9678.
16. Hagmann P, et al. (2008) Mapping the structural core of human cerebral cortex. *PLoS Biol* 6:e159.
17. Drew PJ, Duyn JH, Golanov E, Kleinfeld D (2008) Finding coherence in spontaneous oscillations. *Nat Neurosci* 11:991–993.
18. Fair DA, et al. (2008) The maturing architecture of the brain's default network. *Proc Natl Acad Sci USA* 105:4028–4032.
19. Seeley WW, et al. (2007) Dissociable intrinsic connectivity networks for salience processing and executive control. *J Neurosci* 27:2349–2356.
20. Kelly CA, Uddin LQ, Biswal BB, Castellanos FX, Milham MP (2008) Competition between functional brain networks mediates behavioral variability. *NeuroImage*, 39:527–537.
21. Fox MD, Snyder AZ, Vincent JL, Raichle ME (2007) Intrinsic fluctuations within cortical systems account for intertrial variability in human behavior. *Neuron* 56:171–184.
22. He BJ, et al. (2007) Breakdown of functional connectivity in frontoparietal networks underlies behavioral deficits in spatial neglect. *Neuron* 53:905–918.
23. Gibson EJ (1963) Perceptual learning. *Annu Rev Psychol* 14:29–56.
24. Crist RE, Kapadia MK, Westheimer G, Gilbert CD (1997) Perceptual learning of spatial localization: Specificity for orientation, position, and context. *J Neurophysiol* 78:2889–2894.
25. Van Essen DC (2005) A population-average, landmark- and surface-based (PALS) atlas of human cerebral cortex. *NeuroImage* 28:635–662.
26. Gilbert CD, Sigman M (2007) Brain states: Top-down influences in sensory processing. *Neuron* 54:677–696.
27. Sylvester CM, Shulman GL, Jack AI, Corbetta M (2007) Asymmetry of anticipatory activity in visual cortex predicts the locus of attention and perception. *J Neurosci* 27:14424–14433.
28. Sestieri C, et al. (2008) Independence of anticipatory signals for spatial attention from number of nontarget stimuli in the visual field. *J Neurophysiol* 100(2):829–838.
29. Bisley JW, Goldberg ME (2003) Neuronal activity in the lateral intraparietal area and spatial attention. *Science* 299:81–86.
30. Corbetta M, Shulman GL (2002) Control of goal-directed and stimulus-driven attention in the brain. *Nat Rev Neurosci* 3:201–215.
31. Bressler SL, Tang W, Sylvester CM, Shulman GL, Corbetta M (2008) Top-down control of human visual cortex by frontal and parietal cortex in anticipatory visual spatial attention. *J Neurosc* 28:10056–10061.
32. Dosenbach NU, et al. (2006) A core system for the implementation of task sets. *Neuron* 50:799–812.
33. Shulman GL, et al. (1997) Common blood flow changes across visual tasks: II. Decreases in cerebral cortex. *J Cognit Neurosci* 9:648–663.
34. Raichle ME, et al. (2001) A default mode of brain function. *Proc Natl Acad Sci USA* 98:676–682.
35. Weissman DH, Roberts KC, Visscher KM, Woldorff MG (2006) The neural bases of momentary lapses in attention. *Nat Neurosci* 9:971–978.
36. Shulman GL, Astafiev SV, McAvoy MP, d'Avossa G, Corbetta M (2007) Right TPJ deactivation during visual search: Functional significance and support for a filter hypothesis. *Cereb Cortex* 17:2625–2633.
37. Tootell RBH, et al. (1998) The retinotopy of visual spatial attention. *Neuron* 21:1409–1422.
38. Reynolds JH, Chelazzi L (2004) Attentional modulation of visual processing. *Annu Rev Neurosci* 27:611–647.
39. Damoiseaux JS, et al. (2006) Consistent resting-state networks across healthy subjects. *Proc Natl Acad Sci USA* 103:13848–13853.
40. Granger CWJ (1969) Investigating causal relations by econometric models and cross-spectral methods. *Econometrica* 37:424–438.
41. He BJ, Snyder AZ, Zempel JM, Smyth MD, Raichle ME (2008) Electrophysiological correlates of the brain's intrinsic large-scale functional architecture. *Proc Natl Acad Sci USA* 105:16039–16044.
42. Nir Y, et al. (2008) Interhemispheric correlations of slow spontaneous neuronal fluctuations revealed in human sensory cortex. *Nat Neurosci* 11:1100–1108.
43. Miller KJ, Weaver KE, Ojemann JG (2009) Direct electrophysiological measurement of human default network areas. *Proc Natl Acad Sci USA* 106:12174–12177.
44. Deco G, Jirsa V, McIntosh AR, Sporns O, Kötter R (2009) Key role of coupling, delay, and noise in resting brain fluctuations. *Proc Natl Acad Sci USA* 106:10302–10307.
45. Grill-Spector K, Kushnir T, Hendler T, Malach R (2000) The dynamics of object-selective activation correlate with recognition performance in humans. *Nat Neurosci* 3:837–843.
46. Buckner RL, Andrews-Hanna JR, Schacter DL (2008) The brain's default network. Anatomy, function, and relevance to disease. *Ann N Y Acad Sci* 1124:1–38.
47. Monto S, Palva S, Voipio J, Palva JM (2008) Very slow EEG fluctuations predict the dynamics of stimulus detection and oscillation amplitudes in humans. *J Neurosci* 28:8262–8272.
48. Ghosh A, Rho Y, McIntosh AR, Kötter R, Jirsa VK (2008) Noise during rest enables the exploration of the brain's dynamic repertoire. *PLoS Comp Bio* 4:e1000196.
49. Honey CJ, Kötter R, Breakspear M, Sporns O (2007) Network structure of cerebral cortex shapes functional connectivity on multiple time scales. *Proc Natl Acad Sci USA* 104:10240–10245.
50. Albert NB, Robertson EM, Miall RC (2009) The resting human brain and motor learning. *Curr Bio* 19:1023–1027.
51. Canals S, Beyerlein M, Merkle H, Logothetis NK (2009) Functional MRI evidence for LTP-induced neural network reorganization. *Curr Bio* 19:398–403.
52. Leopold DA, Murayama Y, Logothetis NK (2003) Very slow activity fluctuations in monkey visual cortex: Implications for functional brain imaging. *Cereb Cortex* 13:422–433.
53. Buzsáki G, Draguhn A (2004) Neuronal oscillations in cortical networks. *Science* 304:1926–1929.
54. Fries P (2005) A mechanism for cognitive dynamics: Neuronal communication through neuronal coherence. *Trends Cogn Sciences* 9:474–480.
55. Vanhatalo SJ, et al. (2004) Infraslow oscillations modulate excitability and interictal epileptic activity in the human cortex during sleep. *Proc Natl Acad Sci* 101:5053–5057.
56. Canolty RT, et al. (2006) High gamma power is phase-locked to theta oscillations in human neocortex. *Science* 313:1626–1628.
57. Sigman M, et al. (2005) Top-down reorganization of activity in the visual pathway after learning a shape identification task. *Neuron* 46:823–835.
58. Brandt P (2009) Markov-Switching Bayesian Vector Autoregression Models Package (MSBVAR). Available at http://cran.r-project.org/web/packages/MSBVAR/index.html. Accessed September 16, 2009.
59. R Development Core Team (2008) *R: A Language and Environment for Statistical Computing.* (Vienna, Austria) R Foundation for Statistical Computing. Available at http://www.R-project.org. Accessed September 16, 2009.

Lewis et al.

NEUROSCIENCE